

BRIEF REPORT

Glacier as a source of novel polyethylene terephthalate hydrolases

Xiaoyan Qi¹  | Mukan Ji²  | Chao-Fan Yin¹  | Ning-Yi Zhou¹  |
Yongqin Liu^{2,3,4} 

¹State Key Laboratory of Microbial Metabolism, Joint International Research Laboratory of Metabolic and Developmental Sciences, and School of Life Sciences and Biotechnology, Shanghai Jiao Tong University, Shanghai, China

²Center for Pan-third Pole Environment, Lanzhou University, Lanzhou, China

³State Key Laboratory of Tibetan Plateau Earth System, Resources and Environment (TPESRE), Institute of Tibetan Plateau Research, Chinese Academy of Sciences, Beijing, China

⁴University of Chinese Academy of Sciences, Beijing, China

Correspondence

Ning-Yi Zhou, State Key Laboratory of Microbial Metabolism, Joint International Research Laboratory of Metabolic and Developmental Sciences, and School of Life Sciences and Biotechnology, 800 Dongchuan Road Shanghai, Shanghai Jiao Tong University, Shanghai 200240, China.
Email: ningyi.zhou@sjtu.edu.cn

Yongqin Liu, Center for Pan-third Pole Environment, Lanzhou University, Lanzhou 730000; State Key Laboratory of Tibetan Plateau Earth System, Resources and Environment (TPESRE), Institute of Tibetan Plateau Research, Chinese Academy of Sciences; University of Chinese Academy of Sciences, Beijing, China.
Email: yql@lzu.edu.cn

Funding information

Major Research plan of the National Natural Science Foundation of China, Grant/Award Number: 91851207; National Natural Science Foundation of China, Grant/Award Numbers: 42171138, 918512; The Seed Industry Revitalization Project of Guangdong Province, Grant/Award Number: 23050202; Second Tibetan Plateau Scientific Expedition and Research Program (STEP), Grant/Award Number: 2019QZKK0503; the National Key Research and Development Plans, Grant/Award Number: 2021YFC2300904

Abstract

Polyethylene terephthalate (PET) is a major component of microplastic contamination globally, which is now detected in pristine environments including Polar and mountain glaciers. As a carbon-rich molecule, PET could be a carbon source for microorganisms dwelling in glacier habitats. Thus, glacial microorganisms may be potential PET degraders with novel PET hydrolases. Here, we obtained 414 putative PET hydrolase sequences by searching a global glacier metagenome dataset. Metagenomes from the Alps and Tibetan glaciers exhibited a higher relative abundance of putative PET hydrolases than those from the Arctic and Antarctic. Twelve putative PET hydrolase sequences were cloned and expressed, with one sequence (designated as GlacPETase) proven to degrade amorphous PET film with a similar performance as *Is*PETase, but with a higher thermostability. GlacPETase exhibited only 30% sequence identity to known active PET hydrolases with a novel disulphide bridge location and, therefore may represent a novel PET hydrolases class. The present work suggests that extreme carbon-poor environments may harbour a diverse range of known and novel PET hydrolases for carbon acquisition as an environmental adaptation mechanism.

INTRODUCTION

Plastic contamination is a global concern, over 6300 tons of plastic waste are generated annually worldwide, nearly 80% of which is accumulated in the environment

(Geyer et al., 2017). Large-sized plastic items can break up to form microplastics, which are easily transported naturally by atmospheric (Chen et al., 2020) and aquatic circulation (Li et al., 2020). These microplastic contaminants are globally present, even in remote

Xiaoyan Qi and Mukan Ji contributed equally to this study.

© 2023 Applied Microbiology International and John Wiley Sons & Ltd.

pristine areas including deep ocean, Polar environments, and mountain glaciers (Zhang et al., 2019). Polyethylene terephthalate (PET) is one of the most commonly used plastics due to its excellent mechanical and thermal properties, making it a major component of microplastic contamination globally. Its environmental degradation is mainly by microorganisms, with a wide range of enzymes with PET degradation activities (PET hydrolases) being reported, including cutinases, esterases, lipases, and so on (Kawai et al., 2020). PET hydrolases have been identified in a wide range of microorganisms including actinobacteria, bacteroides, and proteobacteria (Kawai, 2021). Some of these microorganisms can degrade PET for carbon and energy sources (Tanasupawat et al., 2016). Several PET hydrolases have been extensively investigated for their potential commercial applications, but the role of microbial PET degradation in the natural environment has been greatly overlooked, particularly in carbon-poor (oligotrophic) environments where PET as a highly carbon-rich molecule may play a key role in microbial carbon cycling.

Environmental bacteria such as *Ideonella sakaiensis* can use PET as a carbon source at ambient temperature (30°C; Bornscheuer, 2016). This capacity can be particularly important for oligotrophic environments such as glacier ecosystems. Thus, identifying ambient temperature PET hydrolases in such environments could provide additional insights into the survival mechanism of microorganisms in extreme environments. Furthermore, the glacier ecosystem is subjected to environmental stresses including strong UV radiation and dramatic temperature fluctuation, which enhance PET chemical weathering (Montazer et al., 2018; Sørensen et al., 2021), thus facilitating the subsequential microbial degradation. PET has been identified in global glaciers, which is recognised as a major xenobiotic contaminant (Parolini et al., 2021; Zhang et al., 2021). If left untreated, PET can be frozen in ice and stored for thousands of years impairing ecosystem health. Thus, it is vital to understand the fate of PET in the glacial environment. Glacial harbours a wide range of microorganisms performing diverse metabolic functions (Liu et al., 2022b). Currently, we know little about the PET degradation capacity of cold-adapted microorganisms. PET degradation could be advantageous for glacier-dwelling microorganisms by providing the edge for their survival in a carbon-poor environment. In addition, due to the unique composition of glacial microbiomes, glacial microorganisms may encode PET-degrading enzymes with distinct functional properties compared with their temperate counterparts.

To identify potential PET hydrolases from glacial environments, we further updated a recently published glacier gene and genome catalogue (Liu et al., 2022b), which now contains over 62,595,715 genes from

208 metagenomes and 952 cultivated bacterial genomes from global glaciers. As many as 414 putative PET hydrolase hits were obtained from this database using a collection of curated PET hydrolase sequences as queries. In total 12 of them were expressed, one of which was demonstrated to show exceptional activity against PET nanoplastics. Its activity was comparable with *IsPETase* but with a higher thermostability possibly due to the presence of a disulphide bridge at a novel location in its structure. Our results demonstrate that glacier is a new source for the bioprospecting of novel PET hydrolases and possibly other enzymes with potential for industrial applications.

EXPERIMENTAL PROCEDURES

Databases used in the present study

The glacier metagenome and genome data used were based on the database published previously (Liu et al., 2022b) with an additional 123 metagenome and 69 genomes from other non-Tibetan glaciers. Thus, the used dataset contains 208 metagenomes from global glacier habitats (Table S1) and the genomes of 952 cultured isolates (Table S2) in total (Bellas et al., 2020; Franzetti et al., 2016; Hauptmann et al., 2017; Trivedi et al., 2020; Zhang et al., 2020). These metagenomes are from snow, ice, and cryoconite (a mixture of mineral and organic material covering glacial ice). The sequences were quality controlled using the Trim Galore (https://www.bioinformatics.babraham.ac.uk/projects/trim_galore/), assembled using the MEGAHIT (version 1.1.3; Li et al., 2015), and genes were predicted from contigs ≥ 500 bp using Prodigal as described previously (Hyatt et al., 2010). For reads that failed to be assembled, they were pooled from different samples and co-assembled using the MEGAHIT (version 1.1.3; Li et al., 2015), and the resulting contigs ≥ 500 bp were further predicted using Prodigal. The relative abundances of the predicted genes were calculated using Salmon (v0.13.1) and expressed as transcript per Kilobase of ORF per Million mapped reads (TPM). As the present study was on genomic DNA, we renamed this as read-based TPM (RTPM). As the mapping was only performed using sequencing reads of a sample to its predicted ORFs, the abundance of those ORFs from cultivated genomes and co-assembled contigs was not calculated.

Bioinformatics identification of candidate PET hydrolases from glacier microbiome

After removing identical sequences, 35 PET hydrolase reference sequences (Buchholz et al., 2022) were

downloaded from the plastics-active enzymes database and aligned with Clustal Omega (Sievers et al., 2011). Then, based on the alignment results of these sequences, a profile HMM was built using the “build” function of the HMMER package (hmmer.org/). The predicted genes from glacier habitats were analysed by the “hmmsearch” function of the HMMER package. This ended with 403 metagenome-originated and 11 cultured isolates-originated sequences being identified. These sequences were combined with the reference sequences without dereplication and then aligned using muscle (Edgar, 2004). A phylogenetic tree was built using FastTree with the GTR model and Gamma distribution (Price et al., 2010), with the tree being visualised and annotated using iTOL (Letunic & Bork, 2019). Based on the “hmmsearch” score, the top 20 sequences (clustered in two clades) with the highest E-value ranking were selected. Each top E-value ranked sequence in other clades was also selected (five sequences in total). These 25 sequences and the sequences used to construct the HMM model were phylogenetically analysed again. Finally, 12 complete candidate PET hydrolases that were less similar to each other (based on the prodigal prediction with the code partial = 00) were selected manually for further functional validation.

Molecular cloning and protein expression of putative PET hydrolases

The signal peptides of the 12 putative PET hydrolases were predicted by SignalP (Almagro Armenteros et al., 2019) and were excluded in the subsequent gene synthesis. The genes were commercially synthesized with codon optimisation before being cloned into the *Hind*III (5' end) and *Bam*HI (3' end) sites of the pUC19 and the corresponding constructs were transformed into *E. coli* BL21 (DE3). The nucleotide sequences of the 12 candidates with codon optimisation were provided in Table S4. The cells were cultured in Lysogeny broth (LB) with 100 µg/mL ampicillin at 37°C. When the optical density at 600 nm (OD₆₀₀) reached 0.6–0.8, expression was induced by 0.2 mM isopropyl-β-D-thiogalactopyranoside for 16 h at 16°C. Cells were harvested by centrifugation, resuspended in lysis buffer (20 mM Tris-HCl, pH 8, 300 mM NaCl), and then disrupted by ultrasonication before the lysate was collected by centrifugation at 10,000 × g for 30 min.

After preliminary activity screening, three promising candidates (4–1, 6–9, and 9–6) PET hydrolases were subsequently cloned into pET-28a (+) for expression in *E. coli* BL21 (DE3). The cells were cultured in LB with 50 µg/mL kanamycin. The expression induction, cell collection, and preparation of crude enzyme were the same as described above.

Preliminary activity screening with *p*-nitrophenyl butyrate and bis (2-hydroxyethyl) terephthalate as substrates

Preliminary screening of the 12 candidates was performed using *p*-nitrophenyl butyrate (*p*NPB) as a substrate. Reactions were initiated by adding 50 µL of the crude enzyme into 150 µL 10 mM *p*NPB and then was incubated for 15 min at room temperature (25°C). To quantify the product *p*-nitrophenol, the absorbance at 410 nm was measured using a Microplate reader (BioTeK Instruments, Inc, USA). The activity of 12 candidates on bis (2-hydroxyethyl) terephthalate (BHET) was determined using the following method. Briefly, 200 µL of the crude enzyme was added into 200 µL 0.4% BHET solutions, followed by incubation at 37°C for 12 h. The reaction was terminated by adding an equal volume of acetonitrile. Then, the supernatant obtained by centrifugation was filtered using a 0.22 µm filter for HPLC analysis (see below).

Secondary screening with PET nanoplastics as substrates

Amorphous PET film (0.25 mm thickness) was purchased from Goodfellow Cambridge, Ltd. PET stock solutions were prepared by dissolving 0.1 g of PET film into 10 mL 1,1,1,3,3,3-hexafluoro-2-propanol. Then, 1 mL of the crude enzyme was incubated with 10 µL PET stock solutions at 37°C for 24 h. PET nanoplastics were generated at the moment when PET stock solutions were loaded into the buffer. The reaction termination and product detection were the same as those described earlier.

Protein expression and purification of GlacPETase and *Is*PETase

Since the expression product of GlacPETase in *E. coli* BL21 (DE3) was predominantly insoluble, the gene encoding Lactates was then subcloned into the *Eco*RI (5' end) and *Not*I (3' end) sites of pET-32a through fusion to the N-terminal TrxA-coding sequence. Meanwhile, a TEV protease recognition site was added between the genes *trx*A and *glac*PETase to allow for subsequent removal of the TrxA-tag. Then, the constructed plasmid was transformed into *E. coli* BL21 trxB (DE3). Cells were cultured in LB with 100 µg/mL ampicillin at 20°C for 48 h, then harvested and lysed as described previously.

The supernatant was purified by Ni-NTA chromatography. To remove the TrxA-tag and imidazole, purified proteins (46.8 kDa) were digested using TEV protease at 4°C overnight in a dialysis bag. The digested

proteins were purified by Ni-NTA chromatography again and the mature GlacPETase (28.0 kDa) was in the flow-through liquid. Expression and purification of *Is*PETase were performed as reported previously (Han et al., 2017). The obtained proteins were confirmed through SDS-PAGE (Figure S1).

Biochemical characterisation of GlacPETase

The standard activity assay for GlacPETase was performed using *p*NPB as a substrate at 1 mM concentration in 0.1 M Tris-HCl buffer (pH = 8.0). Reactions were initiated by adding 10 μ L of GlacPETase (1 mg/mL) into 190 μ L of the substrate. After incubation for 15 min at room temperature (25°C), the released *p*-nitrophenol was quantified. The optimal pH was determined by incubating the samples in 20 mM Tris-HCl buffers at pH = 6.0, 7.0, 8.0, and 9.0. The optimal substrates were determined using 1 mM *p*NP esters with different chain lengths of C₄, C₆, C₈, C₁₀, C₁₂, C₁₄, C₁₆, and C₁₈. In addition, the influence of different metals, solvents, detergents, and inhibitors on the activity of GlacPETase was also evaluated as described in an earlier report (Danso et al., 2018). The optimal temperature was determined by incubating 1 mL of 500 nM GlacPETase with 10 μ L of 1% PET stock solutions at 4°C, 16°C, 20°C, 30°C, 37°C, and 55°C for 24 h.

The melting temperatures of GlacPETase and *Is*PE-Tase were determined using the Thermofluor assay as reported (Eiamthong et al., 2022) with some modifications. Briefly, 0.2 μ L of Sypro orange (Sigma-Aldrich) was loaded into 25 μ L of purified enzyme (1 mg/mL). Then, the samples were tested on a Real-time PCR (CFX Connect, Bio-Rad, USA).

For the determination of GlacPETase activity on PET film, amorphous PET films were cut into 6 mm diameter sheets using a hole punch. The sheet was placed in a 1.5 mL Eppendorf tube with 300 μ L of GlacPETase (50, 100, 200, 300, and 500 nM) in 20 mM Tris-HCl, 300 mM NaCl buffer at pH 8. The hydrolysis reactions were carried out at 30°C for 48 h. The methods for termination of reaction and product detection were the same as those described previously. In addition, the digested PET films were collected, washed with water, 0.5% SDS, and ethanol sequentially, dried at 50°C for 12 h, and coated with gold (Au) for observation under scanning electron microscopy (SEM, S3400II, Hitachi, Japan).

HPLC analysis

Standard terephthalic acid (TPA), mono (2-hydroxyethyl) terephthalate (MHET), and BHET were purchased from Aladdin Co., Ltd. Identification and quantification of these compounds were performed with

reverse-phase high-performance liquid chromatography (HPLC, e2695, Waters, USA), equipped with a C18 reversed-phase column (5 μ m, 4.6 \times 250 mm, Agilent, USA). The mobile phases were methanol and water containing 0.1% acetic acid. The elution profile was 35% of methanol for 20 min and the effluent was monitored at the wavelength of 240 nm.

Multiple sequence alignment and sequence similarity network (SSN)

By using the enzyme function initiative enzyme similarity tool (EFI-EST; Gerlt et al., 2015), amino acid sequences of GlacPETase and 67 identified PET hydrolases were subjected to construct the SSN with a threshold of $1e^{-10}$. Cytoscape was used to visualise the network (Shannon et al., 2003). The accessions of 67 PET hydrolases analysed in this study are summarised in the Plastics-Active Enzymes Database (Buchholz et al., 2022). Then, six representative PET hydrolases and GlacPETase were subjected to multiple sequence alignment with MAFFT-linsi (version 7; Katoh et al., 2002), shown by ESPript (version 3.0; Robert & Gouet, 2014).

Structure prediction and molecular dynamics simulations

The structure of GlacPETase was predicted by AlphaFold2 (Jumper et al., 2021). The structures of GlacPETase together with *Is*PE-Tase (6EQE; Austin et al., 2018) and Tfcut2 (4CG1; Roth et al., 2014) were visualised by PyMOL (version 2.5.4). Molecular dynamics simulations were performed by employing GRO-MACS 2021 (Tan et al., 2022) using the AMBER99SB force field (Hornak et al., 2006). Proteins were immersed in the TIP3P water octahedron box. The unbalanced charge in the system was neutralised by adding suitable counterions (Na⁺ and Cl⁻). The system was energetically minimised using the steepest descent algorithm, and then continuously equilibrated in the *NVT* and *NPT* ensemble throughout 100 ps, and the heavy atoms were restrained with a force constant of 1000 KJ mol⁻¹ nm⁻¹. The free production run was carried out for 30 ns using an *NPT* ensemble at 300 K (26°C) and 340 K (66°C), respectively, and the time step was 2 fs.

RESULTS

Phylogeny of candidate PET hydrolases in glacier microbiome

After extensive filtering, 403 and 11 putative PET hydrolases were identified from glacier metagenomes

and isolated genomes, respectively (Figure 1A). The phylogeny of the PET hydrolases identified was associated with their taxonomy origin and the region where the sequences were recovered, instead of by their habitats. These sequences originated from 77 glacier-related samples, accounting for over 38% of the samples investigated ($n = 208$). These samples were distributed in 24 glaciers covering ice, snow, and cryoconite habitats, but more frequently from snow (89% of the 28 snow samples, Figure 1B) than ice (37% of the 90 ice samples) and cryoconite (24% of the 90 cryoconite samples). Of the samples with putative

PET hydrolases identified, snow demonstrated the highest PET hydrolases richness ($n = 6.7 \pm 11$, One-Way ANOVA, $p < 0.001$), and decreased in the order of ice ($n = 5.2 \pm 5.2$), and cryoconite ($n = 3.0 \pm 1.9$). BLAST search affiliated these putative PET hydrolases with Proteobacteria (67% of the 403 sequences, Figure 1C), followed by Actinobacteria (17%), Gemmatimonadetes (5%), and Deinococcus-Thermus (4%). Most of the candidate PET hydrolase sequences were locally present, and we did not identify any sequences that are present in all four regions investigated (the Antarctic, Arctic, Alps, and Tibetan Plateau), with only

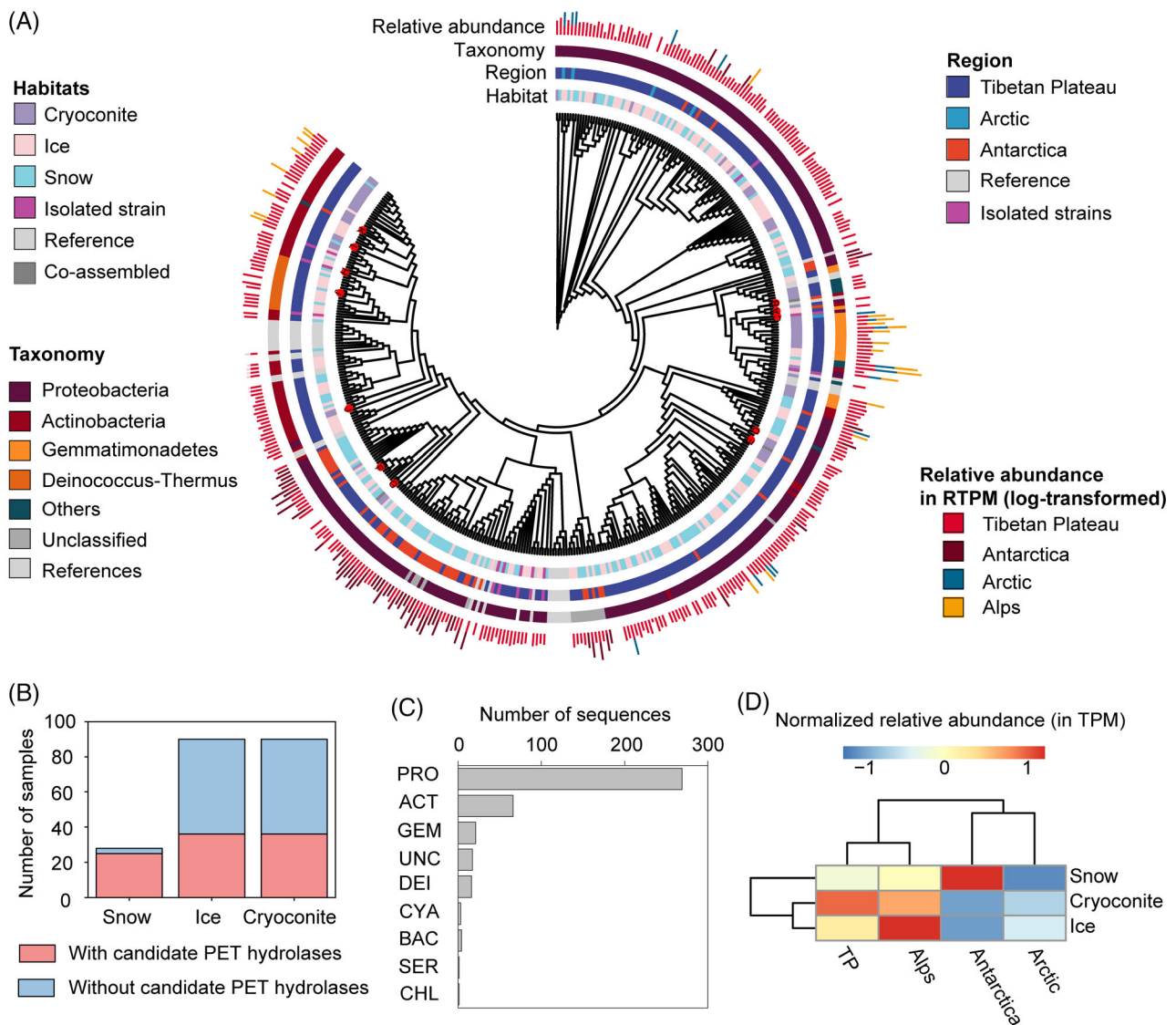


FIGURE 1 Phylogeny of the identified candidate polyethylene terephthalate (PET) hydrolase and its distribution patterns. (A) The phylogenetic relationships of the identified candidate PET hydrolase with reference sequences. Their habitats, regions, taxonomy, and relative abundance are indicated by the outer rings, stars represent sequences cloned and expressed. (B) The number of samples with candidate PET hydrolase identified for each habitat. (C) The taxonomy composition of candidate PET hydrolases. (D) The relative abundance of candidate PET hydrolase for each habitat-region pair. Stars represent sequences cloned and expressed. Co-assembled means the genes were predicted from contigs that are assembled from multiple samples; therefore, the habit information is lost. PRO, proteobacteria; ACT, actinobacteria; BAC, bacteroidetes; CHL, chloroflexi; CYA, cyanobacteria; DEI, deinococcus-thermus; GEM, gemmatimonadetes; SER, Candidatus Sericytochromatia bacterium; UNC, unclassified.

68 putative PET hydrolases being identified from more than one region (17% of the 403 sequences, Figure 1A). The relative abundance of putative PET hydrolases ranged from 2.2×10^5 (the Arctic) to 1.0×10^6 transcripts per million reads (RTPM, the Alps, Figure 1D). Snow harboured a higher relative abundance of PET hydrolases in Antarctic glaciers, while cryoconite and ice had higher relative abundances of putative PET hydrolases in the Tibetan and Alps glaciers, respectively.

Screening of candidate PET hydrolases for PET hydrolysis activity

Twelve candidate PET hydrolases were selected, cloned into a pUC19 vector, and expressed in *E. coli* BL21 (DE3) for function confirmation. For preliminary screening, *p*NPB and BHET were used as substrates because these two small molecules were more susceptible to hydrolysis by hydrolases, narrowing the scope of subsequent searches, as they were used in previous

studies (Han et al., 2023). The crude enzymes of Candidate_C, Candidate_D, and Candidate_J showed activity on *p*NPB and BHET (Figure 2A,B). Among these three candidates, candidate C was from a cultured isolate, which is classified as a novel species within *Pseudomonas*. However, no product was detected when using PET nanoplastics as the substrate. This was speculated to be the consequence of low protein expression, which is insufficient to hydrolyze the PET nanoplastics. Subsequently, these three promising candidates were cloned into pET-28a (+) for a higher expression in *E. coli* BL21 (DE3). As a result, the crude enzyme of Candidate_C exhibited hydrolytic activity on PET nanoplastics, producing TPA and MHET (Figure 2C). Henceforth, the Candidate_C identified from the glacier microbiome was designated GlacPETase for further study.

The activity of GlacPETase against amorphous PET films was tested. After incubating at 30°C for 48 h, products including TPA, MHET, and BHET were detected (Figure 3A). The optimal protein concentration of GlacPETase for the hydrolysis of PET film was

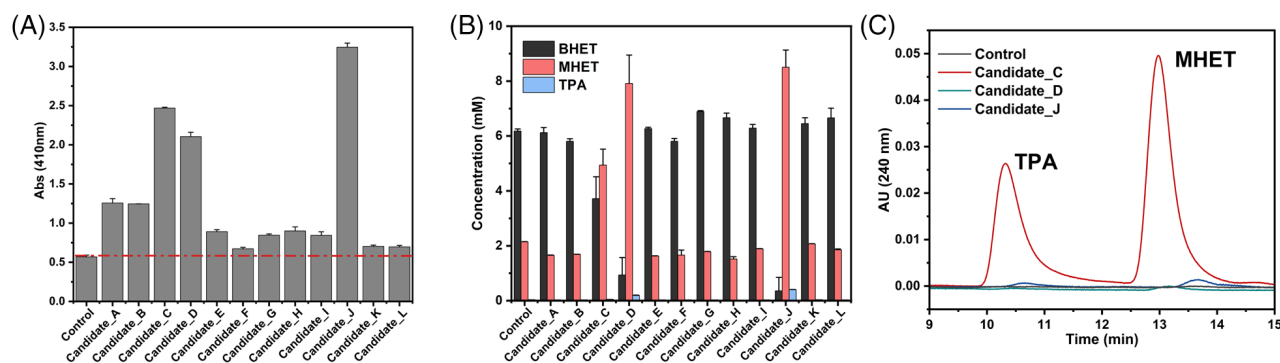


FIGURE 2 Experimental screening of Polyethylene terephthalate (PET) hydrolases from glacier microbiome. (A) Preliminary screening of 12 candidates constructed in pUC19 using *p*-nitrophenyl butyrate as a substrate. The absorbance at 410 nm after reactions are shown. (B) Preliminary screening of 12 candidates constructed in pUC19 with BHET as a substrate. The BHET residue, MHET produced and TPA produced in supernatant after reactions are shown. (C) Secondary screening of three candidates constructed in pET-28a (+) using PET nanoplastics as substrates. Liquid chromatograms of supernatants after reaction are shown.

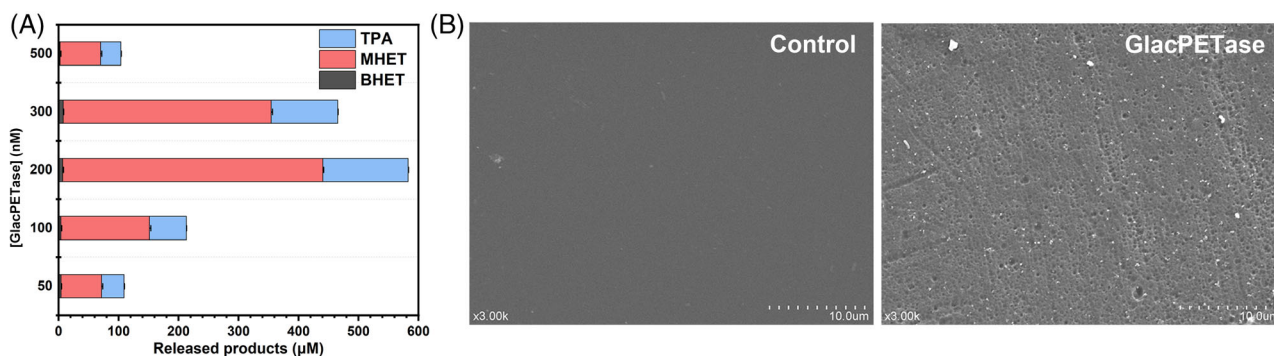


FIGURE 3 Purified GlacPETase activity on amorphous polyethylene terephthalate (PET) films. (A) Products formed after co-incubation of GlacPETase with PET films at different protein concentrations. (B) Scanning electron microscope image of PET film surface after incubating with buffer-only control and with purified GlacPETase.

200 nM. MHET was the major product, with a low quantity of TPA and BHET being also detected. After incubation, the surface of PET film treated by GlacPETase was rougher and exhibited small pits (Figure 3B,C), further confirming the activity of GlacPETase against PET films.

Enzymatic properties of GlacPETase

The optimal pH of GlacPETase is 8.0 (Figure S2A), a relative alkaline value. GlacPETase showed hydrolytic activity on *p*NP esters of different chain lengths (Figure S2B). The activity of GlacPETase against *p*NPB was significantly inhibited by 10 mM of Zn^{2+} , and Mg^{2+} ions, 1 mM DTT, 10% DMF, and 1% SDS (Figure S2C–F). The thermofluor assay indicated that the T_m of GlacPETase was 56°C, higher than *Is*PETase (49°C, Figure 4A). The optimal temperatures for GlacPETase and *Is*PETase with PET nanoplastics as substrates were both 30°C (Figure 4B), but their activity

differed at other temperatures. The total concentrations of the released products by GlacPETase were higher at 37°C than that at 16°C, in contrast to *Is*PETase which exhibited a higher activity at 16°C than that at 37°C.

Molecular dynamics simulations were performed in a 30 ns time scale for *Is*PETase and GlacPETase (Figure 4C,D). The root mean square deviation (RMSD) is used to quantify the structural changes of protein, further reflecting the stabilisation of the protein during molecular dynamics simulations. The RMSD of non-hydrogen atoms computed for these two proteins revealed that both enzymes exhibited steady and remained close to their original structure at 300 K (26°C). At 340 K (66°C), the RMSD of GlacPETase followed a similar trend to that at 300 K whereas the RMSD of *Is*PETase increased. This is another indication that GlacPETase is more thermally stable than *Is*PETase, consistent with the results of the T_m values and the varied activities on PET nanoplastics at different temperatures.

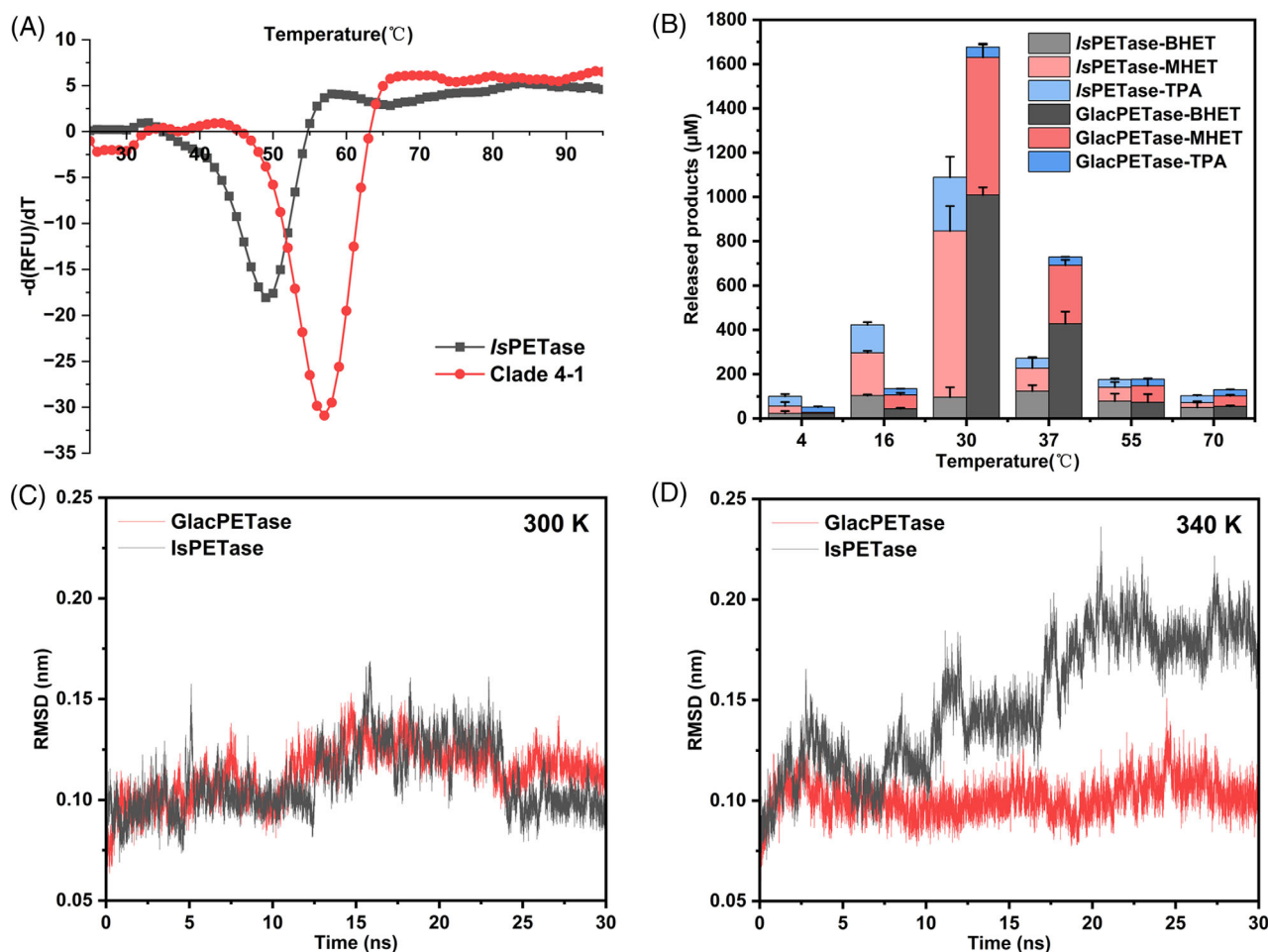


FIGURE 4 Temperature properties of GlacPETase. (A) Comparison of the melting temperature of GlacPETase and *Is*PETase. (B) Products released after co-incubation of GlacPETase or *Is*PETase at different temperatures with polyethylene terephthalate nanoplastics. The RMSD trajectories of *Is*PETase and GlacPETase at 300 K (C) and 340 K (D).

Sequence and structural features of GlacPETase

The full-length sequence of GlacPETase contains 285 amino acids with an N-terminal signal peptide of 25 aa. The molecular weight of mature GlacPETase is predicted to be 28.0 kDa and its isoelectric point (pI) is predicted to be 9.49. In the alignment of GlacPETase with 67 functionally identified PET hydrolases, the maximum identity was only 30.48% with Enzyme 504 (Figure S3), a PET hydrolase from *Caldimonas taiwanensis* + D57 (Erickson et al., 2022). The associations of GlacPETase with the 67 functionally confirmed PET hydrolases were visualised by a SSN (Figure 5A). The SSN had five clusters and eight singletons. The vast majority (50/68) of PET hydrolases were grouped into a single cluster due to their high sequence similarity, while GlacPETase was singled out as a separate node (Figure 5A).

Based on AlphaFold2 prediction, GlacPETase belongs to the canonical α/β hydrolases with a similar structure to several reported PET hydrolases (Figure 5C). Although the catalytic triad (Ser147-His227-Asp196) in GlacPETase is completely conserved, there are some noteworthy structural differences between GlacPETase and other PET hydrolases. GlacPETase exhibited an extra α -helix each at three positions, respectively: near the catalytic center and in front of the seventh and ninth β -sheets (Figure 5C), whereas one less α -helix at the N-terminus of GlacPETase (Figure 5C). However, the most notable of the differences is that the single disulphide bond in GlacPETase was located at the N-terminus observed from the predicted structure (Figure 5C). It was proposed in earlier studies that PET hydrolases can be divided into Type I and Type II, represented by Tfcut2 and *Is*PETase (Joo et al., 2018), respectively. Type I PET hydrolases including LCC (Sulaiman et al., 2012), Tfcut2 (Furukawa et al., 2019), and Cut190 (Miyakawa et al., 2015) have only one disulphide bond at the C-terminus, while the type II including Mors1 (Blázquez-Sánchez et al., 2022), PE-H (Bollinger et al., 2020), and *Is*PETase (Yoshida et al., 2016) has an additional disulphide bond near the catalytic center (Joo et al., 2018; Figure 5B,C). Here, the location of the disulphide bond of GlacPETase was distinct from either of the two types of PET hydrolases (Figure 5C).

DISCUSSION

We identified 414 putative PET hydrolases from glacial habitats, suggesting that PET hydrolases are widespread globally even in pristine environments. A previous study has recovered a PET hydrolase from the Antarctic with maximum activity at ambient temperature (25°C; Blázquez-Sánchez et al., 2022), further

confirming the presence of PET hydrolases in cold environments. Most of the snow metagenomes contained putative PET hydrolase sequences, followed by ice, and cryoconite (Figure 1B). This is consistent with the order of increasing carbon concentration in glacier habitats (Liu et al., 2022a). In addition, the relative abundance of putative PET hydrolases was also the highest in the Alps, followed by the Tibetan Plateau, while their relative abundance was relatively lower in the Antarctic and Arctic glaciers. This order is consistent with the level of human activity, that is, the Alps and Tibetan glaciers are closer to human activities.

PET hydrolases exhibited strong taxonomy conservation, while habitats played little role. This is consistent with the taxonomy conservation reported from putative PET hydrolases from terrestrial and marine environments (Danso et al., 2018; Gambarini et al., 2021). PET hydrolases from the global ocean were dominantly Pseudomonadales-origin (Alam et al., 2020) or Bacteroidetes-origin (Danso et al., 2018). Here, we also identified a high PET hydrolase diversity from Actinobacteria, potentially due to their higher environmental adaptability against strong UV radiation and low temperature (Xie & Pathom-Aree, 2021). *Deinococcus-Thermus* was also predicted to host a wide variety of putative PET hydrolases (Figure 1C), which has also been reported in a genome sequence-based study (Gambarini et al., 2021). *Deinococcus-Thermus* is extremely radiation-tolerant (Slade & Radman, 2011), which is widespread in glacial environments. Thus, Actinobacteria and *Deinococcus-Thermus* PET hydrolases may be extremely valuable for PET degradation in areas with strong UV radiation, such as the Tibetan Plateau and Polar regions.

Several studies have searched metagenome for putative PET hydrolases. A previous study on global ocean metagenomes revealed 68 putative PET hydrolases from 416 metagenomes (Alam et al., 2020); a blast-based search against 7375 terrestrial metagenomes identified 27 putative PET hydrolases (Karunatillaka et al., 2022). The lower number of putative PET hydrolases identified previously from the metagenomes is partly explained by that they targeted *Is*PETase-like with the Dienelactone hydrolase domain, while the present study explored other forms of PET hydrolases as well. This is reflected by Danso et al. (2018), who searched against 25 terrestrial and 108 marine metagenomes for all known PET hydrolase sequences and identified 349 putative PET hydrolases. Therefore, PET hydrolases could be widespread across various natural environments, despite their relative abundance within the metagenomes being low (Figure 1A; Danso et al., 2018). However, not all these putative PET hydrolases exhibited evident (or any) activity towards PET or its substrates (Figure 2), suggesting they may exhibit amino acid composition similarity to known PET hydrolases, but lack key residues

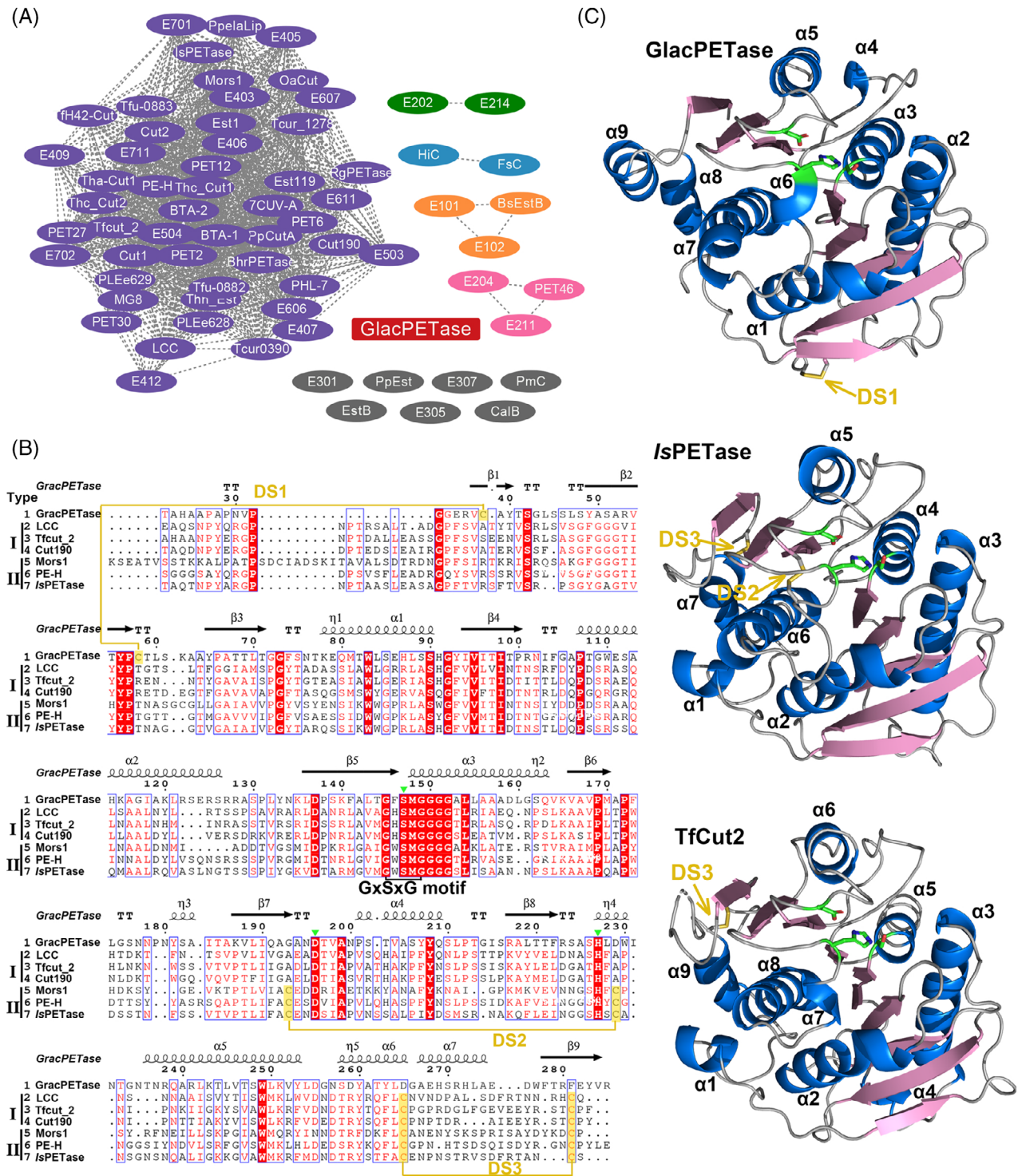


FIGURE 5 Sequence and structural comparison of GlacPETase with other polyethylene terephthalate (PET) hydrolases. (A) A sequence similarity network (SSN) of 67 known PET hydrolases and GlacPETase. GlacPETase was highlighted by a red rectangle. (B) Multiple sequence alignment of GlacPETase with PET hydrolases in different types. Disulphide bonds were highlighted with yellow and the catalytic triad was marked with green triangles. (C) Structural comparison of GlacPETase, IsPETase, and TfCut2.

or binding pockets for proper PET hydrolysis. PET hydrolases belong to a broad enzyme class that has diverse evolutionary origins from lipases, cutinases, carboxylesterases, and other related α/β hydrolases with diverse functions (Danson et al., 2018). Therefore,

these sequence-similar but non-active enzymes could have the capacity to degrade other structurally similar xenobiotics that are important to glacial microorganisms for energy and carbon acquisition, which certainly requires further investigation.

Of the 12 candidate PET hydrolases expressed, three showed activities against BHET and only one activity against amorphous PET film (GlacPETase). This confirms the presence of active PET hydrolases in glacier habitats. The activity of GlacPETase was higher than *IsPETase* at 30°C and 37°C, but lower at 4°C and 16°C (Figure 4B). GlacPETase was obtained from a bacterium isolated from Antarctica and, surprisingly, an enzyme from glacier habitats had higher thermostability than *IsPETase*. The other reported PET hydrolase from the Antarctic seawater (Mors1) had an optimum temperature of 25°C (Blázquez-Sánchez et al., 2022), which is substantially lower than that of GlacPETase. Therefore, the bacteria carrying this enzyme could have been dispersed from warmer environments by atmospheric circulation (Archer et al., 2019). Nevertheless, detectable activity was also observed at a temperature as low as 4°C, this could just provide enough energy to maintain cellular functions. Additionally, GlacPETase mainly releases BHET and MHET as products, while much less TPA compared with *IsPETase* (Figure 4B). This suggests that the two enzymes may have different activity against PET and its oligomers. GlacPETase could be used as an enzyme to depolymerise PET, then its partially degraded products could be further hydrolysed by other oligomers hydrolases (i.e., BHET and MHET hydrolases) to achieve a full degradation of PET.

It is worth noting that the total released products from PET film were highest while the GlacPETase was 200 nM. With the continuous increase of the GlacPETase, the released products decreased (Figure 3A). This phenomenon is known as concentration-dependent inhibition, is evident and common in mesophilic PET hydrolases, regardless of PET depolymerisation efficiency level (Luisana Avilan et al., 2023). One of the explanations for this phenomenon was the inhibitory protein surface overcrowding effect (Baath et al., 2021). Increased protein concentrations lead to protein over-crowding on the surface of the PET film, where lateral interactions between proteins hinder enzyme–substrate binding. As a result, the proportion of proteins in productive conformation declines, resulting in a decrease in product content. However, the exact molecular mechanisms behind this phenomenon have not been thoroughly investigated.

The unique location of the disulphide bond in GlacPETase could make GlacPETase represent a novel PET hydrolases class. Disulphide bonds contribute to the thermal stability of PET hydrolases (Emori et al., 2021; Sulaiman et al., 2014). Based on the melting temperatures comparison between GlacPETase and *IsPETase* (Figure 4A), GlacPETase exhibited a higher thermostability compared with *IsPETase*. Thus, the novel disulphide bond location may be associated with its improved thermostability. However, this may need further experimental clarification. Nevertheless,

this may provide additional hints into the engineering of other PET hydrolases for further improving their thermostability.

CONCLUSION

We obtained 414 putative PET hydrolase sequences from the global glacier metagenome dataset, with one sequence (designated as GlacPETase) successfully cloned and expressed with PET degradation activity. The GlacPETase depolymerised PET film and exhibited higher thermostability compared with *IsPETase*. Multiple sequence comparisons and AlphaFold2 protein structure prediction revealed a novel disulphide bridge location, therefore GlacPETase may represent a novel PET hydrolases class. The present work suggests that glaciers harbour a diverse range of known and novel PET hydrolases, making glaciers a new resource for the bioprospecting of novel enzymes with potential industrial applications.

AUTHOR CONTRIBUTIONS

Xiaoyan Qi: Data curation (equal); investigation (equal); methodology (equal); validation (equal); visualization (equal); writing – original draft (equal). **Mukan Ji:** Data curation (equal); investigation (equal); methodology (equal); validation (equal); visualization (equal); writing – original draft (equal). **Chao-Fan Yin:** Data curation (equal); investigation (equal); methodology (equal); writing – original draft (equal). **Ning-Yi Zhou:** Conceptualization (lead); project administration (lead); resources (lead); supervision (lead); writing – review and editing (lead). **Yongqin Liu:** Conceptualization (lead); funding acquisition (lead); project administration (lead); resources (lead); supervision (lead); writing – review and editing (lead).

ACKNOWLEDGEMENTS

This study was supported by the Second Tibetan Plateau Scientific Expedition and Research Program (STEP) (2019QZKK0503), the Seed Industry Revitalisation Project of Guangdong Province (23050202), the National Key Research and Development Plans (2021YFC2300904), National Natural Science Foundation of China (General Program 42171138 and 918512), and the Major Research plan of the National Natural Science Foundation of China (91851207).

CONFLICT OF INTEREST STATEMENT

The authors declare no conflicts of interest.

DATA AVAILABILITY STATEMENT

The protein sequences of 414 putative PET hydrolases from the global glacier metagenome dataset, the sequence ID, relative abundance, habitat, and classification were provided in Table S3.

ORCID

Xiaoyan Qi  <https://orcid.org/0000-0001-8599-139X>Mukan Ji  <https://orcid.org/0000-0001-8139-2875>Chao-Fan Yin  <https://orcid.org/0000-0002-6905-0909>Ning-Yi Zhou  <https://orcid.org/0000-0002-0917-5750>Yongqin Liu  <https://orcid.org/0000-0003-2876-7484>

REFERENCES

- Alam, I., Aalismaail, N., Martin, C., Kamau, A., Guzmán-Vega, F.J., Jamil, T. et al. (2020) Rapid evolution of plastic-degrading enzymes prevalent in the global ocean. *bioRxiv*.
- Almagro Armenteros, J.J., Tsirigos, K.D., Sønderby, C.K., Petersen, T.N., Winther, O., Brunak, S. et al. (2019) SignalP 5.0 improves signal peptide predictions using deep neural networks. *Nature Biotechnology*, 37, 420–423.
- Archer, S.D.J., Lee, K.C., Caruso, T., Maki, T., Lee, C.K., Cary, S.C. et al. (2019) Airborne microbial transport limitation to isolated Antarctic soil habitats. *Nature Microbiology*, 4, 925–932.
- Austin, H.P., Allen, M.D., Donohoe, B.S., Rorrer, N.A., Kearns, F.L., Silveira, R.L. et al. (2018) Characterization and engineering of a plastic-degrading aromatic polyesterase. *Proceedings of the National Academy of Sciences*, 115, E4350–E4357.
- Baath, J.A., Borch, K., Jensen, K., Brask, J. & Westh, P. (2021) Comparative biochemistry of four polyester (PET) hydrolases**. *Chembiochem*, 22, 1627–1637.
- Bellas, C.M., Schroeder, D.C., Edwards, A., Barker, G. & Anesio, A.M. (2020) Flexible genes establish widespread bacteriophage pan-genomes in cryoconite hole ecosystems. *Nature Communications*, 11, 4403.
- Blázquez-Sánchez, P., Engelberger, F., Cifuentes-Anticevic, J., Sonnendecker, C., Griñén, A., Reyes, J. et al. (2022) Antarctic polyester hydrolases degrade aliphatic and aromatic polyesters at moderate temperatures. *Applied and Environmental Microbiology*, 88, e0184221.
- Bollinger, A., Thies, S., Knieps-Grünhagen, E., Gertzen, C., Kobus, S., Höpner, A. et al. (2020) A novel polyester hydrolase from the marine bacterium *Pseudomonas aestusnigri*—structural and functional insights. *Frontiers in Microbiology*, 11, 114.
- Bornscheuer, U.T. (2016) Feeding on plastic. *Science*, 351, 1154–1155.
- Buchholz, P.C.F., Feuerriegel, G., Zhang, H., Perez-Garcia, P., Nover, L.-L., Chow, J. et al. (2022) Plastics degradation by hydrolytic enzymes: the plastics-active enzymes database—PAZy. *Proteins: structure, function, and bioinformatics*, 90, 1443–1456.
- Chen, G., Feng, Q. & Wang, J. (2020) Mini-review of microplastics in the atmosphere and their risks to humans. *Science of the Total Environment*, 703, 135504.
- Danso, D., Schmeisser, C., Chow, J., Zimmermann, W., Wei, R., Leggewie, C. et al. (2018) New insights into the function and global distribution of polyethylene terephthalate (PET)-degrading bacteria and enzymes in marine and terrestrial metagenomes. *Applied and Environmental Microbiology*, 84, e02773.
- Edgar, R.C. (2004) MUSCLE: multiple sequence alignment with high accuracy and high throughput. *Nucleic Acids Research*, 32, 1792–1797.
- Eiamthong, B., Meesawat, P., Wongsatit, T., Jitdee, J., Sangsri, R., Patchsung, M. et al. (2022) Discovery and genetic code expansion of a polyethylene terephthalate (PET) hydrolase from the human saliva metagenome for the degradation and bio-functionalization of PET. *Angewandte Chemie (International Ed in English)*, 61, e202203061.
- Emori, M., Numoto, N., Senga, A., Bekker, G.J., Kamiya, N., Kobayashi, Y. et al. (2021) Structural basis of mutants of PET-degrading enzyme from *Saccharomonospora viridis* AHK190 with high activity and thermal stability. *Proteins*, 89, 502–511.
- Erickson, E., Gado, J.E., Avilán, L., Bratti, F., Brizendine, R.K., Cox, P.A. et al. (2022) Sourcing thermotolerant poly(ethylene terephthalate) hydrolase scaffolds from natural diversity. *Nature Communications*, 13, 7850.
- Franzetti, A., Tagliaferri, I., Gandolfi, I., Bestetti, G., Minora, U., Mayer, C. et al. (2016) Light-dependent microbial metabolisms drive carbon fluxes on glacier surfaces. *ISME Journal*, 10, 2984–2988.
- Furukawa, M., Kawakami, N., Tomizawa, A. & Miyamoto, K. (2019) Efficient degradation of poly(ethylene terephthalate) with *Thermobifida fusca* cutinase exhibiting improved catalytic activity generated using mutagenesis and additive-based approaches. *Scientific Reports*, 9, 16038.
- Gambarini, V., Pantos, O., Kingsbury, J.M., Weaver, L., Handley, K.M. & Lear, G. (2021) Phylogenetic distribution of plastic-degrading microorganisms. *mSystems*, 6, e01112–e01120.
- Gerlt, J.A., Bouvier, J.T., Davidson, D.B., Imker, H.J., Sadkhin, B., Slater, D.R. et al. (2015) Enzyme function initiative-enzyme similarity tool (EFI-EST): a web tool for generating protein sequence similarity networks. *Biochimica et Biophysica Acta*, 1854, 1019–1037.
- Geyer, R., Jambeck, J.R. & Law, K.L. (2017) Production, use, and fate of all plastics ever made. *Science Advances*, 3, e1700782.
- Han, X., Liu, W., Huang, J.-W., Ma, J., Zheng, Y., Ko, T.-P. et al. (2017) Structural insight into catalytic mechanism of PET hydrolase. *Nature Communications*, 8, 2106.
- Han, Y., Dierkes, R.F. & Streit, W.R. (2023) Metagenomic screening of a novel PET esterase via In vitro expression system. *Methods in Molecular Biology*, 2555, 167–179.
- Hauptmann, A.L., Sicheritz-Ponten, T., Cameron, K.A., Baelum, J., Plichta, D.R., Dalggaard, M. et al. (2017) Contamination of the Arctic reflected in microbial metagenomes from the Greenland ice sheet. *Environmental Research Letters*, 12, 074019.
- Hornak, V., Abel, R., Okur, A., Strockbine, B., Roitberg, A. & Simmerling, C. (2006) Comparison of multiple Amber force fields and development of improved protein backbone parameters. *Proteins*, 65, 712–725.
- Hyatt, D., Chen, G.L., Locascio, P.F., Land, M.L., Larimer, F.W. & Hauser, L.J. (2010) Prodigal: prokaryotic gene recognition and translation initiation site identification. *BMC Bioinformatics*, 11, 119.
- Joo, S., Cho, I.J., Seo, H., Son, H.F., Sagong, H.-Y., Shin, T.J. et al. (2018) Structural insight into molecular mechanism of poly(ethylene terephthalate) degradation. *Nature Communications*, 9, 382.
- Jumper, J., Evans, R., Pritzel, A., Green, T., Figurnov, M., Ronneberger, O. et al. (2021) Highly accurate protein structure prediction with AlphaFold. *Nature*, 596, 583–589.
- Karunatillaka, I., Jaroszewski, L. & Godzik, A. (2022) Novel putative polyethylene terephthalate (PET) plastic degrading enzymes from the environmental metagenome. *Proteins*, 90, 504–511.
- Katoh, K., Misawa, K., Kuma, K. & Miyata, T. (2002) MAFFT: a novel method for rapid multiple sequence alignment based on fast Fourier transform. *Nucleic Acids Research*, 30, 3059–3066.
- Kawai, F. (2021) Emerging strategies in polyethylene terephthalate hydrolase research for biorecycling. *ChemSusChem*, 14, 4115–4122.
- Kawai, F., Kawabata, T. & Oda, M. (2020) Current state and perspectives related to the polyethylene terephthalate hydrolases available for biorecycling. *ACS Sustainable Chemistry & Engineering*, 8, 8894–8908.
- Letunic, I. & Bork, P. (2019) Interactive tree of life (iTOL) v4: recent updates and new developments. *Nucleic Acids Research*, 47, W256–W259.
- Li, D., Liu, C.M., Luo, R., Sadakane, K. & Lam, T.W. (2015) MEGA-HIT: an ultra-fast single-node solution for large and complex metagenomics assembly via succinct de Bruijn graph. *Bioinformatics*, 31, 1674–1676.

- Li, Y., Zhang, H. & Tang, C. (2020) A review of possible pathways of marine microplastics transport in the ocean. *Anthropocene Coasts*, 3, 6–13.
- Liu, Y., Fang, P., Guo, B., Ji, M., Liu, P., Mao, G. et al. (2022a) A comprehensive dataset of microbial abundance, dissolved organic carbon, and nitrogen in Tibetan plateau glaciers. *Earth System Science Data*, 14, 2303–2314.
- Liu, Y., Ji, M., Yu, T., Zaugg, J., Anesio, A.M., Zhang, Z. et al. (2022b) A genome and gene catalog of glacier microbiomes. *Nature Biotechnology*, 40, 1341–1348.
- Luisana Avilan, B.R.L., Koenig, G., Zahn, M., Allen, M.D., Oliveira, L., Clark, M. et al. (2023) Concentration-dependent inhibition of mesophilic PETases on poly(ethylene terephthalate) can be eliminated by enzyme engineering. *ChemSusChem*, 16, e202202277.
- Miyakawa, T., Mizushima, H., Ohtsuka, J., Oda, M., Kawai, F. & Tanokura, M. (2015) Structural basis for the Ca²⁺-enhanced thermostability and activity of PET-degrading cutinase-like enzyme from *Saccharomonospora viridis* AHK190. *Applied Microbiology and Biotechnology*, 99, 4297–4307.
- Montazer, Z., Habibi-Najafi, M.B., Mohebbi, M. & Oromiehei, A. (2018) Microbial degradation of UV-pretreated low-density polyethylene films by novel polyethylene-degrading bacteria isolated from plastic-dump soil. *Journal of Polymers and the Environment*, 26, 3613–3625.
- Parolini, M., De Felice, B., Lamonica, C., Cioccarelli, S., Crosta, A., Diolaiuti, G. et al. (2021) Macroplastics contamination on glaciers from Italian Central-Western Alps. *Environmental Advances*, 5, 100084.
- Price, M.N., Dehal, P.S. & Arkin, A.P. (2010) FastTree 2—approximately maximum-likelihood trees for large alignments. *PLoS One*, 5, e9490.
- Robert, X. & Gouet, P. (2014) Deciphering key features in protein structures with the new ENDscript server. *Nucleic Acids Research*, 42, W320–W324.
- Roth, C., Wei, R., Oeser, T., Then, J., Föllner, C., Zimmermann, W. et al. (2014) Structural and functional studies on a thermostable polyethylene terephthalate degrading hydrolase from *Thermobifida fusca*. *Applied Microbiology and Biotechnology*, 98, 7815–7823.
- Shannon, P., Markiel, A., Ozier, O., Baliga, N.S., Wang, J.T., Ramage, D. et al. (2003) Cytoscape: a software environment for integrated models of biomolecular interaction networks. *Genome Research*, 13, 2498–2504.
- Sievers, F., Wilm, A., Dineen, D., Gibson, T.J., Karplus, K., Li, W. et al. (2011) Fast, scalable generation of high-quality protein multiple sequence alignments using Clustal omega. *Molecular Systems Biology*, 7, 539.
- Slade, D. & Radman, M. (2011) Oxidative stress resistance in *Deinococcus radiodurans*. *Microbiology and Molecular Biology Reviews*, 75, 133–191.
- Sørensen, L., Groven, A.S., Hovsbakken, I.A., Del Puerto, O., Krause, D.F., Sarno, A. et al. (2021) UV degradation of natural and synthetic microfibers causes fragmentation and release of polymer degradation products and chemical additives. *Science of the Total Environment*, 755, 143170.
- Sulaiman, S., Yamato, S., Kanaya, E., Kim, J.J., Koga, Y., Takano, K. et al. (2012) Isolation of a novel cutinase homolog with polyethylene terephthalate-degrading activity from leaf-branch compost by using a metagenomic approach. *Applied and Environmental Microbiology*, 78, 1556–1562.
- Sulaiman, S., You, D.J., Kanaya, E., Koga, Y. & Kanaya, S. (2014) Crystal structure and thermodynamic and kinetic stability of metagenome-derived LC-cutinase. *Biochemistry*, 53, 1858–1869.
- Tan, C., Jung, J., Kobayashi, C., Torre, D.U.L., Takada, S. & Sugita, Y. (2022) Implementation of residue-level coarse-grained models in GENESIS for large-scale molecular dynamics simulations. *PLoS Computational Biology*, 18, e1009578.
- Tanasupawat, S., Takehana, T., Yoshida, S., Hiraga, K. & Oda, K. (2016) *Ideonella sakaiensis* sp. nov., isolated from a microbial consortium that degrades poly(ethylene terephthalate). *International Journal of Systematic and Evolutionary Microbiology*, 66, 2813–2818.
- Trivedi, C.B., Stamps, B.W., Lau, G.E., Grasby, S.E., Templeton, A.S. & Spear, J.R. (2020) Microbial metabolic redundancy is a key mechanism in a sulfur-rich glacial ecosystem. *Msystems*, 5, e00504-20.
- Xie, F. & Pathom-Aree, W. (2021) Actinobacteria from desert: diversity and biotechnological applications. *Frontiers in Microbiology*, 12, 765531.
- Yoshida, S., Hiraga, K., Takehana, T., Taniguchi, I., Yamaji, H., Maeda, Y. et al. (2016) A bacterium that degrades and assimilates poly(ethylene terephthalate). *Science*, 351, 1196–1199.
- Zhang, B.L., Chen, T., Guo, J.M., Wu, M.H., Yang, R.Q., Chen, X.M. et al. (2020) Microbial mercury methylation profile in terminus of a high-elevation glacier on the northern boundary of the Tibetan plateau. *Science of the Total Environment*, 708, 135226.
- Zhang, Y., Gao, T., Kang, S., Allen, S., Luo, X. & Allen, D. (2021) Microplastics in glaciers of the Tibetan plateau: evidence for the long-range transport of microplastics. *Science of the Total Environment*, 758, 143634.
- Zhang, Y., Gao, T., Kang, S. & Sillanpää, M. (2019) Importance of atmospheric transport for microplastics deposited in remote areas. *Environmental Pollution*, 254, 112953.

SUPPORTING INFORMATION

Additional supporting information can be found online in the Supporting Information section at the end of this article.

How to cite this article: Qi, X., Ji, M., Yin, C.-F., Zhou, N.-Y. & Liu, Y. (2023) Glacier as a source of novel polyethylene terephthalate hydrolases. *Environmental Microbiology*, 1–12. Available from: <https://doi.org/10.1111/1462-2920.16516>